Model-free readout-error mitigation for quantum expectation values

Ewout van den Berg, Zlatko K. Minev, and Kristan Temme IBM Quantum, T.J. Watson Research Center Yorktown Heights, NY, USA (Dated: July 6, 2022)

Measurements on current quantum-hardware are subject to hardware imperfections that lead to readout-errors. These errors manifest themselves as a bias in quantum expectation values. Here, we propose a method to remove this bias from the expectation values of Pauli observables. No specific form of the noise is assumed, other than requiring that it is 'weak'. We apply a method that forces the bias in the expectation value to appear as a multiplicative factor irrespective of the actual noise process. This factor can be measured directly and removed, at the cost of an increase in the sampling complexity for the observable. A bound relating the error in the expectation value to the sample complexity is derived.

I. INTRODUCTION

A significant fraction of the proposed algorithms [1– 8] for near-term quantum devices can be cast in to the following form. First a reasonably shallow quantum circuit is applied, and then the expectation value of an observable is measured on the output state by sampling. The general assumption in this scenario is that proper quantum error-correction [9–12] is not available on these near-term devices. The coherence time and other errors limit the size of the calculation that can be performed. These noise parameters therefore dictate how shallow the circuit has to be. In-spite of these restrictions to the computational model, the hardware noise still generates a bias in the resulting expectation values. It is the goal of error-mitigation techniques to remove this bias and produce more accurate expectation values. For errors that occur during the application of the quantum circuit several error-mitigation protocols have been proposed [13– 21] and also experimentally implemented [22, 23]. The removal of the bias in the expectation value comes at the additional cost of repeating the computation with altered parameters, by an increased sampling cost, or other classical post-processing steps.

In this work we consider the mitigation of readout errors that occur during the final measurement step of the computation. We focus on the computation of the expectation values of Pauli observables. Since Pauli matrices constitute a Hermitian matrix basis, they can represent any observable [24]. Moreover, any observable, such as local Hamiltonians, that can be expanded in a polynomial number of Pauli matrices can be estimated efficiently by measuring the expectation values of Pauli observables, due to the linearity of the expectation value.

After a quantum circuit has been applied the Pauli observable is measured in the computational basis. Any Pauli observable is rotated in to the computational basis by applying single-qubit Clifford gates. The ideal measurement output of a quantum circuit in the computational basis is described in terms of a probability distribution p. The readout errors can be represented by a classical noise map [25–27]. For an n-qubit system, this map is given by a 2^n -by- 2^n left-stochastic matrix A where

entry $A_{i,j}$ denotes the probability of measuring i instead of j for $i, j \in \{0, 1\}^n$. The noisy probability distribution \tilde{p} measured on the device is related to the ideal output by $\tilde{p} = Ap$.

A direct approach to mitigate the effect of read-out errors has frequently been to first measure the output frequencies \hat{r}_x for different bit strings x and then to apply matrix inverse A^{-1} to these frequencies [3, 26, 28]. Directly inverting this matrix is of course only feasible when the system size is small, or when it can be assumed that the noise factorizes so that the stochastic matrix can be inverted for every qubit individually. Experiments have shown, however, that the noise is correlated [29] so that a product approximation to the stochastic matrix can not be assumed to hold in practice. Several approaches have been proposed to deal with this more difficult scenario [30–32] as well as with other settings [32–34]. Recently, a readout error-mitigation scheme has been proposed and experimentally implemented [35] with a formal performance guarantee for a correlated noise model with a sampling overhead that depends on the noise strength. The noise map does not need to be explicitly inverted and the model can be concisely represented using $\mathcal{O}(\text{poly}(n))$ parameters.

Here, we propose a readout-error mitigation method that is motivated by work on quantum benchmarking protocols [36, 37]. The method does not make an explicit assumption about the actual physical noise model when measuring Pauli observables. Pauli matrices are transformed into diagonal Z - Pauli matrices in the computational basis by single-qubit rotations prior to measurement. The protocol is introduced in Section II and randomizes the output channel by applying uniform Pauli bit flips prior to measurement. The action of the Pauli flip is then accounted for by updating the Z - Pauli diagonals accordingly. In Section III we show that this randomization transforms the action of an arbitrary noise map A in to a multiplicative factor for the measured Pauli observable. The factor can be measured directly in the absence of the quantum circuit and the mitigated Pauli expectation value is obtained by dividing out this factor. The division by this factor increases the variance of the estimated observable, which leads to a higher sampling overhead to retain the same sampling error. The magnitude of this factor depends on the underlying noise strength. as shown in Section IV. Simulations in Section V indicate that the method scales reasonably to larger system sizes in the presence of moderate noise. For the readout-error mitigation protocol the error from the initial state preparation is neglected. A generalization of the basic protocol with Pauli-randomization after the input, as explained in Section II. allows us to estimate individual components of the Pauli transfer matrix.

II. METHOD

Consider a system of n qubits and order the set of Pauli operators such that P_q denotes a unique Pauli operator for $q \in \mathcal{P} := [0, 4^{n-1}]$. The Pauli-z operators are assigned indices $\mathcal{Z} := [0, 2^{n-1}]$ such that the Pauli string representation $(\{I,Z\}^{\otimes n})$ is in lexicographical order when read from right to left (the operator on the first qubit changes fastest). The identity operator has index zero, and we define singleton $\mathcal{I} = \{0\}$. Finally, we denote the set of indices corresponding to Pauli-x operators by \mathcal{X} .

We can express any unitary operator U in terms of its Pauli transfer matrix T_U . Element $i, j \in \mathcal{P}$ of the transfer matrix is defined as

$$T_U(i,j) = \frac{1}{2^n} \text{Tr}(P_i(UP_jU^{\dagger})), \tag{1}$$

such that

$$U\rho U^{\dagger} = \frac{1}{2^n} \sum_{p,q \in \mathcal{P}} T_U(p,q) \text{Tr}[P_q \rho] P_p \tag{2}$$

for any state ρ . Given the initial state

$$\rho_0 = |0\rangle\langle 0| = 2^{-n}(I + \sigma_z)^{\otimes n} = 2^{-n} \sum_{j \in \mathcal{Z}} P_j, \quad (3)$$

we are interested in measuring two quantities. The first quantity estimates the Pauli-z component P_i in the final state $\rho = U \rho_0 U^{\dagger}$, namely

$$Tr(P_i \rho) = \sum_{i \in \mathcal{Z}} T_U(i, j). \tag{4}$$

The second quantity considers an individual element of the Pauli transfer matrix $T_U(i,j)$ with indices $i,j \in \mathcal{Z}$. Throughout we assume that all measurements are done in the computational basis and that the initial state is as given in (3). This means that we can only access Pauliz components in (1) and (4). In order to access other components we can augment unitary U with appropriate basis changes, if needed.

Estimation protocol

In order to estimate the quantities of interest we run various instances of the circuit given in Figure 1(a). The

$$|0\rangle \longrightarrow P_p \longrightarrow C \longrightarrow P_q \longrightarrow$$

$$|0\rangle \longrightarrow C \longrightarrow P_q \longrightarrow P_q \longrightarrow$$

$$|0\rangle \longrightarrow P_q \longrightarrow P_q \longrightarrow$$

$$|0\rangle \longrightarrow P_q \longrightarrow P_q \longrightarrow$$

$$|0\rangle \longrightarrow P_q \longrightarrow P_q \longrightarrow$$

FIG. 1. Illustration of circuits used for the estimation of error-mitigated averages. The most general circuit (a) includes Pauli operations indexed by integers p and q. Choosing p=0 gives $P_0=I$, and leads to the simplified circuit in (b). Further choosing C = I gives the circuit in (c).

circuit is parameterized by Pauli indices p and q, and operator C (or the circuit that implements it). We assume that identity operators are simplified, which can result in the circuits given in Figure 1(b) and 1(c). The general procedure for acquiring is then as follows:

Protocol AcquireData(S_p , S_q , C, N) 1: Initialize an empty dataset D

- for i = 1, ..., N do
- Uniformly sample p from S_p 3:
- 4:
- Uniformly sample q from S_q Run the circuit in Figure 1(a) with parameters p, q and operator C
- Record measurement m and add (p, q, m) to \mathcal{D}
- 7: return \mathcal{D}

We represent each measurement as an integer m such that the least-significant bit in the binary representation corresponds to the first qubit and the most-significant bit to the last qubit. For classical post-processing of the data we define the function

$$f(\mathcal{D}, i, j) = \frac{1}{|\mathcal{D}|} \sum_{(p,q,m) \in \mathcal{D}} \gamma_{i,q} \gamma_{j,p} H_{m,i}, \tag{5}$$

where $\gamma_{a,b}$ has the value 1 if Paulis P_a and P_b commute and a value of -1 otherwise. The scalar value $H_{m,i}$ represents the element at row m and column i of the unnormalized Hadamard matrix given by

$$H = H_2^{\otimes n}$$
 where $H_2 = \begin{bmatrix} 1 & 1 \\ 1 & -1 \end{bmatrix}$. (6)

The protocol for estimating $Tr(P_i\rho)$ in (4) for Pauli-z operator $i \in \mathcal{Z}$ then consists of the following steps:

Protocol 1

- 1. $\mathcal{D}_0 = \text{AcquireData}(\mathcal{I}, \mathcal{X}, I, N)$
- 2. $\mathcal{D}_1 = \text{AcquireData}(\mathcal{I}, \mathcal{X}, U, N)$
- 3. Return estimate $f(\mathcal{D}_1, i, 0) / f(\mathcal{D}_0, i, 0)$

Note that the data acquired in steps 1 and 2 can be reused to evaluate the quantity in step 3 for different values of $i \in \mathcal{Z}$. For simplicity we set the number of samples in each of the two datasets to N. More generally we could choose different numbers of samples for each of these steps. The estimation of $T_U(i,j)$ in (1) for any $i,j \in \mathcal{Z}$ follows a similar approach and is given by:

Protocol 2

- 1. $\mathcal{D}_0 = \text{AcquireData}(\mathcal{I}, \mathcal{X}, I, N)$
- 2. $\mathcal{D}_2 = \text{AcquireData}(\mathcal{X}, \mathcal{X}, U, N)$
- 3. Return estimate $f(\mathcal{D}_2, i, j)/f(\mathcal{D}_0, i, 0)$

As before, the data from steps 1 and 2 can be reused to evaluate $T_U(i,j)$ for various $i,j \in \mathcal{Z}$ in step 3. Since the data acquired in step 1 is independent of the choice of U it can be shared for both protocols and be reused for different operators U. As we describe in more detail, it may be beneficial to replace parameters \mathcal{X} by \mathcal{P} in the data acquisition in some cases.

III. DERIVATION

Starting with some notation, we denote by 1 the vector of all ones of appropriate size, and by e_i the *i*-th column of the identity matrix I, This allows us to express the *i*-th column of Hadamard matrix H as $h_i = He_i$. Further note that H is a symmetric real matrix with inverse $H^{-1} = 2^{-n}H$. It follows from our ordering of the Pauli operators that the top-left 2^n -by- 2^n block of the Pauli transfer matrix T_U contains the transfer coefficients between the Pauli-z operators, and we denote this matrix by τ_U . Next, we define the function Z that maps density operator ρ to a vector of length 2^n containing the weights of each Pauli-z operator:

$$Z(\rho) = \sum_{i \in \mathcal{Z}} \operatorname{Tr}[P_i \rho] e_i.$$

We use an unscaled trace, which means that $Z(\rho_0) = 1$ for the initial state ρ_0 . Applying Z to the conjugation of ρ_0 with operator U satisfies $Z(U\rho_0U^{\dagger}) = \tau_U Z(\rho_0)$. The chosen Pauli ordering also allows us to concisely write the measurement probability vector corresponding to state ρ as $p = H^{-1}Z(\rho)$. We can model measurement errors by applying the transition matrix A, which gives effective probabilities $\tilde{p} = AH^{-1}Z(\rho)$. We later show how to deal with more general readout errors.

In order to see the effect of adding random Pauli operators, define the vector $d_q = \sum_{i \in \mathbb{Z}} \gamma_{i,q} e_i$ of commutation values and corresponding diagonal matrix $D_q = \operatorname{diag}(d_q)$. It holds that $Z(P_q \rho P_q) = D_q Z(\rho)$, and based on properties of the Pauli-x subgroup we have:

$$\mathbb{E}_{p \in \mathcal{X}}\left[\gamma_{i,p} d_p\right] = \mathbb{E}_{p \in \mathcal{X}}\left[\gamma_{i,p} D_p Z(\rho_0)\right] = e_i,$$

for any $i \in \mathcal{Z}$. The Pauli P_p term combined with the scalar $\gamma_{i,p}$ therefore allows us, on average, to zero out all but one of the Pauli-z terms in ρ_0 . The circuit in Figure 1(a) with C = U and Pauli matrices P_p and P_q

has a noisy measurement probability vector that can be written as

$$\tilde{p}_U(p,q) = AHD_q \tau_U D_p Z(\rho_0)$$

Denote $M = HAH^{-1}$ and define the function

$$f_{U,p}(i,j) = \mathbb{E}_q \left[\gamma_{i,q} \gamma_{j,p} h_i^T \tilde{p}_U(p,q) \right]$$

$$= \mathbb{E}_q \left[\gamma_{i,q} \gamma_{j,p} e_i^T H A H^{-1} D_q \tau_U D_p Z(\rho_0) \right]$$

$$= \gamma_{j,p} e_i^T M \operatorname{diag} \left(\mathbb{E}_{q \in \mathcal{X}} \left[\gamma_{i,q} d_q \right] \right) \tau_U D_p \mathbf{1}$$

$$= \gamma_{i,p} M_{i,i} \tau_U D_p \mathbf{1}.$$

We can fix p = 0, which gives $P_p = I$, and define

$$f_U(i) := f_{U,0}(i,\cdot) = M_{i,i}\tau_U \mathbf{1} = M_{i,i} \sum_{j \in \mathcal{Z}} \tau_U(i,j).$$
 (7)

Alternatively we can take the expectation over $p \in \mathcal{X}$:

$$f_U(i,j) := \mathbb{E}_{p \in \mathcal{X}} \left[f_U(i,j) \right] = M_{i,i} \tau_U(i,j).$$

The transfer matrix for the identity operator I is given by $\tau_I(i,j) = \delta_{i,j}$, and it follows that $f_I(i) = M_{i,i}$. The readout-error mitigated values for (4) and (1) are then respectively obtained using scalar division:

$$\frac{f_U(i)}{f_I(i)} = \sum_{j \in \mathcal{Z}} \tau_U(i, j) \quad \text{and} \quad \frac{f_U(i, j)}{f_I(i)} = \tau_U(i, j), \quad (8)$$

whenever $M_{i,i} \neq 0$.

For a more general treatment we can replace Z by a function C that extracts all Pauli coefficients. The restricted transfer matrix τ_U can then be replaced by the full transfer matrix T_U . Ideal noise-free measurements are then obtained by applying a 2^n -by- 4^n linear map with first 2^n columns containing the Hadamard matrix, and the remaining entries zero. In the general setting we can envisage $\operatorname{Tr}(P_k \rho_0) \neq 0$ for some $k \in \mathcal{P} \setminus \mathcal{Z}$. Similarly, it may be possible that the measurements are affected by terms that are not in the Pauli-z group. By adding randomly sampled operators from a Pauli subgroup \mathcal{S} it can be seen that, on average, we filter out all Pauli terms that do not commute with all elements in S. In the specific case where S corresponds to the Pauli-z group that means that we filter out all terms outside this group, since it is a maximally commuting subgroup. For the initial state we can therefore multiply P_p with a random Pauli-z matrix. This is equivalent to sampling p from \mathcal{P} rather than \mathcal{X} . Likewise we can filter out all terms that are not in the Pauli-z group by sampling q from \mathcal{P} . After this we can express the noisy measurement operator as $AH^{-1}\Lambda$, where Λ is a quantum noise channel. This is equivalent to $(AH^{-1}\Lambda H)H^{-1} = A'H^{-1}$, which thus allows us to model quantum noise as a classical noise channel.

IV. ANALYSIS

A. Sample complexity

The goal of protocols 1 and 2 is to estimate the quantities in (8). If we write these quantities in the form x/y,

then we see that the protocols work by generating estimates \hat{x} and \hat{y} and returning \hat{x}/\hat{y} . We now consider the sample complexity of the protocols. That is, what value of N we should choose, such that with probability at least $1-\delta$ the final estimate deviates at most ϵ from the exact value. Before doing so, we first consider the accuracy of the estimate in the case we can estimate x and y up to an error of at most α .

Lemma IV.1. Let x, y be such that $0 \le |x| \le |y| \le 1$. Given estimates \hat{x}, \hat{y} with $|x - \hat{x}| \le \alpha$ and $|y - \hat{y}| \le \alpha$, such that $0 \le \alpha \le |y|/2$. Then

$$\left|\frac{\hat{x}}{\hat{y}} - \frac{x}{y}\right| \le \frac{4\alpha}{y}.$$

Proof. Assume without loss of generality that $x, y \geq 0$. Taking the Taylor-series expansion around zero for sufficiently small α we have in the worst case that

$$\frac{\hat{x}}{\hat{y}} = \frac{x+\alpha}{y-\alpha} = \frac{x}{y} + \left(1 + \frac{x}{y}\right) \sum_{k=1}^{\infty} \left(\frac{\alpha}{y}\right)^k
\leq \frac{x}{y} + \left(1 + \frac{x}{y}\right) \cdot \left(\frac{1}{1-\alpha/y} - 1\right)
\leq \frac{x}{y} + \left(1 + \frac{x}{y}\right) \cdot \left(\frac{\alpha/y}{1-\alpha/y}\right) \leq \frac{x}{y} + \frac{4\alpha}{y}.$$

In the last inequality we use the fact that $x/y \leq 1$, and $1 - \alpha/y \geq 1/2$. A lower bound can be derived similarly to obtain the given result.

With this we can obtain the following sample complexity:

Theorem IV.2. With probability at least $1-\delta$, protocols 1 and 2 respectively estimate (4) and (1) with error at most ϵ for a fixed $i, j \in \mathcal{Z}$ when the number of samples N satisfies

$$N \ge \frac{32\log(4/\delta)}{M_{i,i}^2 \epsilon^2}.$$

Proof. Protocols 1 and 2 acquire data and estimate different quantities using the function in (5). For a fixed i and j, we can view each term in the summation as an independent ± 1 sample from a certain distribution depending on U that marginalizes over Pauli indices p and q. For the error in the estimated quantities, we therefore apply Hoeffding's inequality, which states that, given independent random variables X_i from any distribution over [-1,1], the deviation of $\bar{X} = N^{-1} \sum_{i=1}^{N} X_i$ to the expected value $\mathbb{E}(X)$ satisfies

$$\Pr\left(\left|\bar{X} - \mathbb{E}(X)\right| \ge \alpha\right) \le 2\exp\left(-\frac{1}{2}N\alpha^2\right).$$
 (9)

We want to ensure that probability of deviating from the expectation by α or more, is bounded by $\delta/2$. Using the union bound it then follows that the enumerator and



FIG. 2. Diagonalization masks for 12 qubits, obtained by averaging the outer products of commutation vectors d_q using, from left to right, 30, 100, 1000, and 3000 random $q \in \mathcal{X}$.

denominator are α close to their expectation with probability at least $1 - \delta$. Bounding the failure probability in (9) from above by $\delta/2$ gives the sufficient condition

$$N \ge \frac{2\log(4/\delta)}{\alpha^2}.\tag{10}$$

We now need to choose α such that the final estimate is ϵ accurate. From Lemma IV.1 we see that it suffices to take $4\alpha/y \leq \epsilon$, where $y = f_I(i) = M_{i,i}$. Substituting $\alpha = \epsilon M_{i,i}/4$ in (10) then gives the desired result.

As discussed in more detail in Section IV C, the term $M_{i,i}$ is expected to scale weakly exponential in the weight of the Pauli-z observable with a base that deviates from unity by the magnitude of the noise. The increase in sampling complexity therefore depends on the strength of the noise similar to the quasi-probabilistic noise cancellation method in ref [13].

B. Number of circuit instances

For a given q, the term $D_q M D_q$ can be written as the elementwise product of M and the outer product $d_q d_q^T$. The outer product has the important property that diagonal elements are always one, irrespective of the signs in d_q . For randomly sampled $q \in \mathcal{X}$ or $q \in \mathcal{P}$, each off-diagonal value has an equal chance of being plus or minus one, and therefore has an expected value of zero. When the number of qubits n is small we can iterate over all possible q values and obtain exact diagonalization of M. For larger values of n this becomes intractable and we can therefore only approximately diagonalize M. as illustrated in Figure 2. For calibration we estimate $e_i M \mathbf{1} = M_{i,i} + e_i M (\mathbf{1} - e_i)$. In order to suppress the second term we need to sample sufficiently many circuits instances. For the actual estimate of $M_{i,i}$ itself we simply need to sample sufficiently many times regardless of the circuit instance. At this point we should also remark that the actual procedure depends on measurements from the probability vector $\tilde{p} = AH^{-1}D_qZ(\rho_0)$ and we therefore need to sample each circuit sufficiently many times.

In this section we give bounds on the number of circuit instances we need to estimate $M_{i,i}$ to a given accuracy. Given that we multiply by an approximately diagonal mask, this bound depends in part on the maximum off-diagonal elements in M. We show how this corresponds to properties of the transfer matrix A and study these

properties for different types of transfer matrices. When sampling individual elements of τ_U we need to approximately zero out all but one of the coefficients in $Z(\rho_0)$. We study properties of the Pauli transfer matrix to determine the extend to which we need to shrink these elements. Our final estimates are given by the ratio of two quantities and we therefore consider how the estimation error in these quantities affect the result. Note that through this section we work with the full matrix representation for clarify; as shown in Section II, processing itself is done based on individual elements.

For the the number of circuit instances we need to approximately diagonalize M, we have the following result:

Theorem IV.3. Given k randomly sampled values $q_1, \ldots, q_k \in \mathcal{X}$ and an index set $\mathcal{I} \subseteq [2^n]$. Define

$$\hat{M} = \frac{1}{k} \sum_{\ell=1}^{k} (D_{q_{\ell}} M D_{q_{\ell}}) \quad and \quad \beta = \max_{i \in \mathcal{I}} \sum_{j \neq i} |M_{i,j}|.$$

Then we satisfy $|e_i \hat{M}(\mathbf{1} - e_i)| \le \epsilon$ and $|\hat{M}_{i,i} - M_{i,i}| \le \epsilon$ simultaneously for all $i \in \mathcal{I}$ with probability at least $1 - \delta$ whenever

$$k \ge 2 \frac{\log(2/\delta) + n\log(2) + \log(|\mathcal{I}|)}{\epsilon^2/(1+\beta)^2}.$$
 (11)

Proof. Let i be any element in \mathcal{I} . Given independent random variables X_i from any distribution over [-1,1], then it follows from Hoeffding's inequality that the deviation of $\bar{X} = k^{-1} \sum_{i=1}^{k} X_i$ to the expected value $\mathbb{E}(X)$ satisfies

$$\Pr\left(\left|\bar{X} - \mathbb{E}(X)\right| \ge \epsilon\right) \le 2\exp\left(-\frac{1}{2}k\epsilon^2\right).$$
 (12)

For scaling of the off-diagonal elements we uniformly sample X from $\{-1,1\}$. If we can ensure that each element is scaled by a factor at most ϵ_b , then we have an additive term with magnitude at most $\epsilon_b\beta$ in the estimation of $M_{i,i}$. For the estimation of $M_{i,i}$ itself, we apply (12) with X following an appropriate distribution on [-1,1] and a maximum deviation of ϵ_a . Using a union bound over the off-diagonal elements in the row we obtain the condition

$$2\exp(-\frac{1}{2}k\epsilon_a^2) + 2(2^n - 1)\exp(-\frac{1}{2}k\epsilon_b^2) \le \delta \tag{13}$$

In case $\beta = 0$ we can choose $\epsilon_a = \epsilon$ and let $\epsilon_b \to \infty$. Using a union bound over the rows in \mathcal{I} gives a sufficient number of circuit instances of

$$k \ge \frac{\log(2/\delta) + \log(|\mathcal{I}|)}{\epsilon^2/2}.$$

For the more general case where $\beta \neq 0$ we choose $\epsilon_a = \epsilon_b$, which reduces condition (13) to

$$2^n \exp(-\frac{1}{2}k\epsilon_a^2) = \exp(n\log(2) - \frac{1}{2}k\epsilon_a^2) \le \delta/2.$$
 (14)

In order to satisfy $\epsilon_a + \epsilon_b \beta \leq \epsilon$ we must choose $\epsilon_a \leq \epsilon/(1+\beta)$. Combined with a union bound, obtained by multiplying the left-hand side of (13) by the cardinality of \mathcal{I} , this gives the sample complexity stated in 11.

As an aside, we note that diagonalization of quantum noise channels using Pauli twirls follows exactly the same principle as the one we use for diagonalizing M. A simple modification of Theorem IV.3 can then be used to determine the number of circuits needed to ensure that all off-diagonal noise terms are bounded by ϵ .

C. Example transition matrices

For a given transition matrix A we define corresponding transformed matrix $M = HAH^{-1}$. This can be seen as readout transition matrix for Pauli-z operators. It is easily seen that $M^{-1} = HA^{-1}H^{-1}$ whenever the inverse of A exists. For convex combinations of two error channels, namely $A = \mu A_1 + (1 - \mu)A_2$ with $\mu \in [0, 1]$, we have $M = \mu M_1 + (1 - \mu)M_2$. This straightforwardly generalizes to the convex combination of any number of transition matrices.

As a simple example of a transition matrix, consider the case where the outcome of each qubit is independently flipped with some probability r. The transition matrix for a single qubit is then given by

$$A_i = \begin{pmatrix} 1 - r_i & s_i \\ r_i & 1 - s_i \end{pmatrix}, \tag{15}$$

with r=s. These matrices are then combined into a global transition matrix $A=A_{s_1}\otimes\cdots\otimes A_{s_n}$. The corresponding Pauli readout transition matrix then has a particularly simple structure:

$$HAH^{-1} = \bigotimes_{\ell=1}^{n} (H_2 A_{r_{\ell}} H_2^{-1}) = \bigotimes_{\ell=1}^{n} \begin{bmatrix} 1 & 0 \\ 0 & (1 - 2r_{\ell}) \end{bmatrix}$$
 (16)

In this case, since M is already diagonal, we do not need to shrink the off-diagonal elements. It therefore suffices to choose an arbitrary but fixed value for $q \in \mathcal{X}$ for the circuits, rather than sample it. Choosing q=0 simplifies the resulting circuits. Assume for simplicity that all probabilities r_{ℓ} are equal to r, then it follows from (16) that the diagonal element $M_{i,i}$ is directly related to the weight of the Pauli-z operator P_i . For each σ_z term in P_i we have a multiplicative term (1-2r). The diagonal term for P_i with k non-identity term is then given by $(1-2r)^k$. The term $(1-2r)^k$ is bounded below by 1-2kr, that means that for 30 qubits with 1% probability of a measurement flip, the diagonal elements in M are still at least 0.4. In the noiseless case the bit flip probability is zero and we obtain A=M=I.

The transition matrix for the situation where we only measure zeros is given by $A = e_0 e^T$ with a corresponding matrix $M = e e_0^T$. In case each outcome is measured with equal probability regardless of the state we have $A = 2^{-n} e e^T$ and $M = e_0 e_0^T$. Although not realistic by themselves, these matrices could be used in convex combinations with other transition matrices. A good, but not very realistic, example of a transition matrix that is

perfectly invertible but provides difficulty for our method is the following permutation matrix:

$$A = \begin{bmatrix} \cdot & \cdot & 1 & \cdot \\ 1 & \cdot & \cdot & \cdot \\ \cdot & \cdot & \cdot & 1 \\ \cdot & 1 & \cdot & \cdot \end{bmatrix}, \qquad HAH^{-1} = \begin{bmatrix} 1 & \cdot & \cdot & \cdot \\ \cdot & \cdot & -1 & \cdot \\ \cdot & 1 & \cdot & \cdot \\ \cdot & \cdot & \cdot & -1 \end{bmatrix}$$

In case information we have an approximate inverse \hat{A}^{-1} , we can adjust our scheme to work with $D_q H \hat{A}^{-1} \tilde{p}$ instead of $D_q H \tilde{p}$. This form of preconditioning could help increase the magnitude of the diagonal elements in M or reduce that of the off-diagonal elements but may be computationally expensive. Finally, note that classical multiplication

D. Practical considerations

In most of the discussion so far we have assumed ideal state preparation. Suppose that, instead of $\rho_0 = |0\rangle\langle 0|$, we can only prepare $\tilde{\rho}_0$. For calibration this means that, after diagonalization of M, we obtain the vector

$$(M \odot I)Z(\hat{\rho}_0) = \operatorname{diag}(Z(\hat{\rho}_0))m \tag{17}$$

rather than m. If we assume that state preparation for qubits it independent and that each qubit ℓ is initialized to state $(1-\alpha_\ell)|0\rangle\langle 0|+\alpha|1\rangle\langle 1|=\frac{1}{2}(I+(1-2\alpha_\ell)\sigma_z)$, then we have

$$Z(\hat{\rho}_0)^T = \bigotimes_{\ell} \left(\begin{array}{c} 1 \\ 1 - 2\alpha_{\ell} \end{array} \right).$$

Under this assumption, that means that, if we can estimate the α_{ℓ} values, we can incorporate this information in (17) to better estimate m. Aside from improving calibration, knowledge of $\tilde{\rho}_0$ would also allows us to better estimate of individual elements in the Pauli transfer matrix τ_U . For Pauli observables, however, we could at best obtain a readout-error free estimate of

$$\tau_U Z(\tilde{\rho}_0)$$
,

due to the mixing of terms by τ_U . In case τ_U is diagonal, for instance in benchmarking settings, there is no mixing and readout-error correction simultaneously takes care of state preparation errors without knowledge of $\tilde{\rho}$.

Once the calibration data set has been acquired it can be used to mitigate readout errors for circuits with various U, possibly with basis changes. In practical systems we can expect gradual changes in systemic gate and readout errors. That means that calibration data has a limited lifetime. For error mitigation in the proposed approach we traverse the calibration data whenever we want to compute the correction factor for an individual Pauli-z operator. This approach makes updates to the calibration data set very light weight: we could simply augment the calibration data with time stamps and periodically

add some new data points while retiring data that falls outside the current time window. For approaches based on explicit inversion of the transfer matrix, any such update would amount to regeneration of the entire matrix and its inverse. The computation complexity for updating the correction factor using (5) is linear in the size of the data set. The evaluation of an element in the Hadamard matrix and commutation between two n-qubit Pauli operators both take $\mathcal{O}(n)$ time.

Note that the scalar terms $H_{m,i}$ in (5) could be replaced by elements from any other matrix, say G with $|G_{m,i}| \leq 1$, provided that the (relevant) diagonal elements of GAH^{-1} are sufficiently large.

As mentioned in Section IV, we can only access information about M by sampling from $\tilde{p}=AH^{-1}D_qZ(\rho_0)$ for each instance q. In practice we therefore need to make a tradeoff between the number of circuit instances and the number of samples per circuit. We leave a detailed analysis of this for future work.

V. SIMULATION

We evaluate the performance of the proposed method on a simple quantum circuit consisting of a single $R_y(\alpha_i\theta)$ gate on each qubit, where α_i is a scaling parameter that differs for each qubit, and θ is a global phase. We choose $\alpha_1 = 3$ and $\alpha_i = 0.15$ for all remaining qubits. The Pauli transfer matrix corresponding to $R_y(\theta)$ is given by

$$T_{R_y(\theta)} = \begin{pmatrix} 1 & 0 & 0 & 0\\ 0 & \cos(\theta) & 0 & \sin(\theta)\\ 0 & 0 & 1 & 0\\ 0 & -\sin(\theta) & 0 & \cos(\theta) \end{pmatrix}.$$

When applied to a Pauli-z operator with σ_z components for qubits $i \in \mathcal{I}$, the final weight is given by

$$\prod_{i \in \mathcal{I}} \cos(\alpha_i \theta) \tag{18}$$

We simulate noisy readout by forming a transition matrix A with individual asymmetric bit-flip channels with a larger weight for 1 to 0 transitions. The transition matrix additionally includes correlated readout errors on pairs of qubits. In Figures 3(a)–(c) we illustrate a seven-qubit transition matrix A, the corresponding $M = HAH^{-1}$, as well as the product $A_s^{-1}A$, where A_s is the transition matrix that we would obtain if we would determine the exact bit-flip frequencies for each of the qubits, and form the corresponding transition matrix. The diagonal terms of the aforementioned three matrices, along with the sum of absolute values of the off-diagonal elements in M, are plotted in Figure 3(d).

As a first experiment we consider a 12-qubit system and allow the proposed method to sample 256 circuits and acquire 512 measurements per circuit. For matrix inversion we take the same total number of measurements,

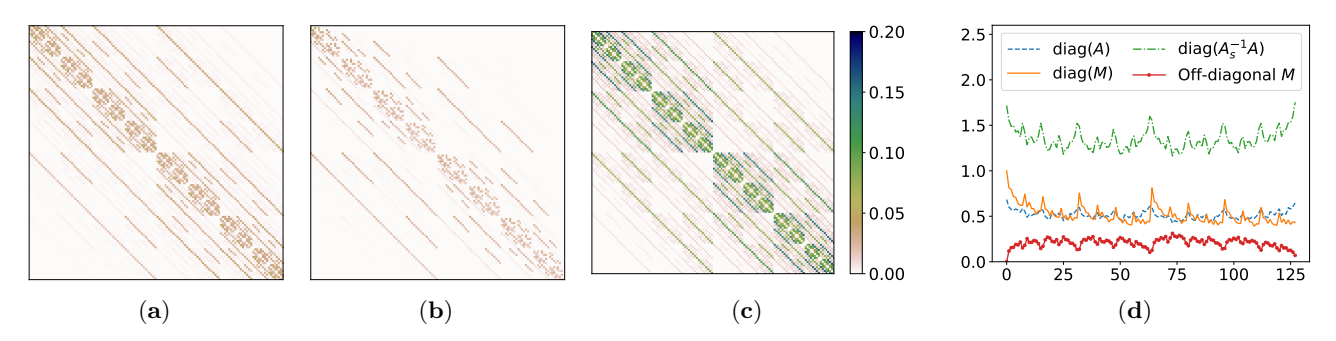


FIG. 3. Magnitude of the off-diagonal matrix entries of (a) transition matrix A, (b) matrix $M = HAH^{-1}$, and (c) matrix $A_s^{-1}A$, where A_s is the single-qubit bit-flip model of A. We zero out the diagonal elements to highlight the off-diagonal structure and relative magnitude of the elements; the diagonal matrix elements are shown in plot (d) along with the sum of absolute values of the off-diagonal elements in M. If the transition matrix A did not include any correlated readout errors, the matrix $A_s^{-1}A$ would be the identity matrix with unit diagonal entries.

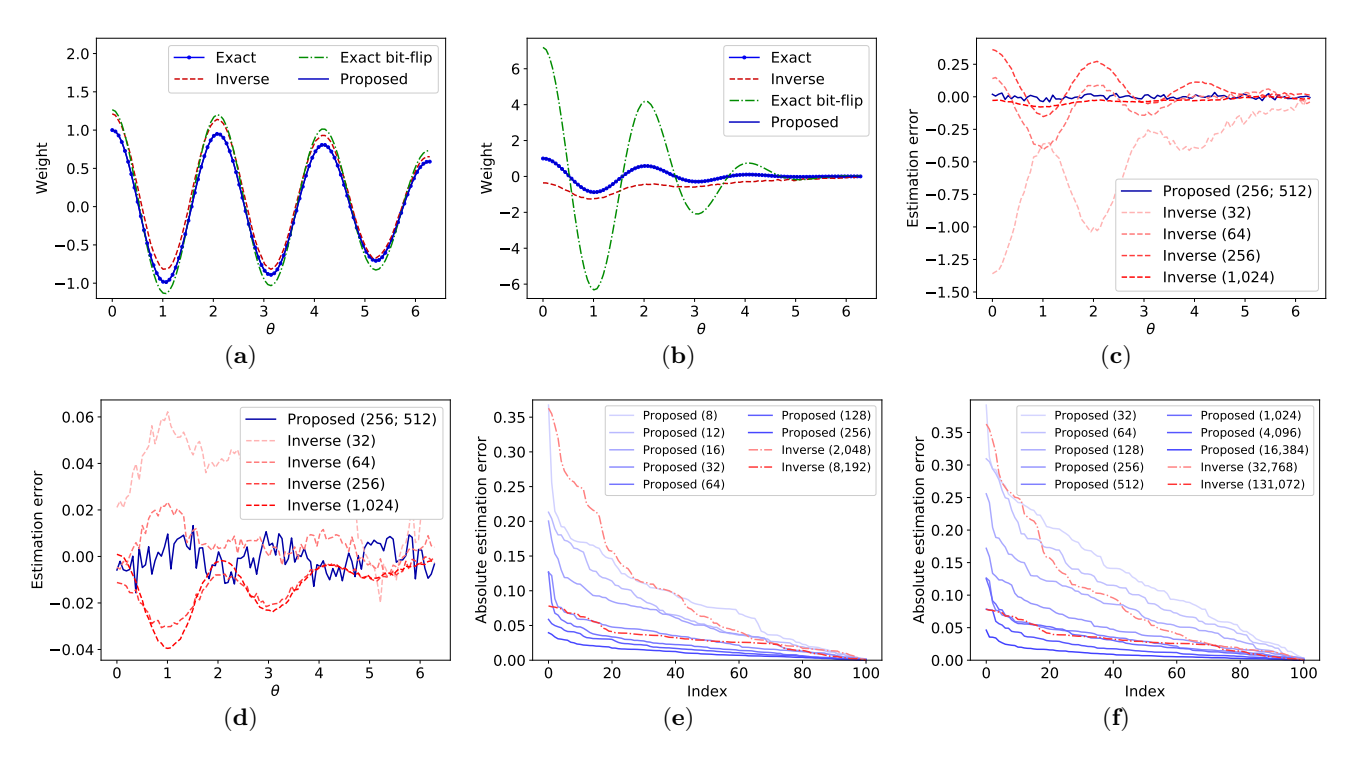


FIG. 4. Simulation results for exact and estimate weights for Pauli-z operators in a twelve-qubit system with (a) a single σ_z term on the first qubit, and (b) all σ_z terms using 256 random circuits and 512 measurement per circuit for the proposed method and the same total number of measurements for the matrix-inversion approach. We evaluate the method for a range of θ values, resulting in different solutions as given by (18). Plots (c) and (d) give the estimation error for the Pauli operators in (b) and (a), respectively, for easy comparison. The proposed method again uses 256 random circuits with 512 measurements each. For the matrix-inversion approach we sample each of the 2^{12} circuits 32 to 1,024 times. Keeping the number of measurements fixed to 512, plot (e) shows the sorted approximation errors over the θ value, for different numbers of circuits. For the inverse approach we show the equivalent number of circuits such that the product gives the total number of measurements. Plot (f) keeps number of circuits in the proposed approach fixed to 32 and varies the number of measurements per circuit. For the inverse approach we list the equivalent number as before.

but spread out over each of the 2,048 columns, each corresponding to a unique circuits, thus giving a maximum of 64 measurements per circuit. The resulting estimates for the weights of Pauli-z operators with σ_z at the first qubit, respectively all qubits are shown in Figures 4(a) and 4(b) for a range of θ values in (18). The estimates obtained using the proposed approach are very close to the

exact solution; so close in fact that the curves are hard to distinguish. Given that the transition matrix contains correlated noise terms, the exact bit-flip approximation can never exactly mitigate the readout noise, as seen from the rather poor performance. Finally, the results based on the inverse of the estimated transition matrix \hat{A} appear to be biases in both settings and relatively lead more

accurate, but still nowhere near the performance of the proposed method. By increasing the number of samples per circuit we can improve the accuracy of the estimates, as illustrated in Figure 4(c) and 4(d). However, even with 32 times as many measurements, the results obtained using matrix inversion are still not as accurate as those obtained using the proposed method. Note that the estimation error for the low-weight Pauli operator in Figure 4(d) is much lower the the weight-n Pauli.

In the next series of experiments we fix the number of circuits for the proposed method to 512 and vary the number of measurements per circuit instance. We sort the resulting estimation errors in magnitude for the different θ values and plot the result in Figure 4(e). We compare the results with those obtained using the matrix-inversion approach, and display the equivalent number of measurements per circuits. Forming the full matrix requires $2^{12} = 2.048$ circuits, which means that the actual number of measurements per circuit is four times lower than the number shown. To match the performance of the proposed method with 32 samples per circuit, the matrix-inversion approach requires an equivalent of 8,192 samples per circuit, which is 128 times as many measurements in total. Similarly, in Figure 4(f) we compare the performance of the methods by fixing the number of circuits to 32 and varying the number of measurements per circuit. The same multiple of measurements is shown in this case.

VI. CONCLUSIONS

In this work we have proposed an efficient method for readout error mitigation in the estimation of Pauli observables. Unlike most existing techniques, the proposed approach does not require any a priori assumptions or model of the readout-error process. The approach is based on the augmentation of quantum circuits with randomly selected Pauli operators and the evaluation of a scalar function based on the measurements obtained using a series of random instances. Readout errors are then mitigated simply by dividing the function value for the quantum circuit of interest by that of the benchmark circuit. The approach works by diagonalizing the readouterror transfer matrix in the Hadamard domain, which makes it trivial to invert. In contrast to many of the existing algorithms, the proposed approach directly estimates the weight of the Pauli-z components in the state (or elements of the Pauli transfer matrix), rather than the distribution of the distribution of measurement values. Our simulations show that the method is capable of mitigating correlated readout error in a twelve-qubit system with very few measurements and circuit instances.

After completion of the manuscript we became aware of the independent work by Chen *et al.* [38] that contains similar ideas as those presented here.

ACKNOWLEDGMENTS

We thank Sergey Bravyi for helpful comments and discussion. This work is supported by the IBM Research Frontiers Institute.

- A. Peruzzo, J. McClean, P. Shadbolt, M.-H. Yung, X.-Q. Zhou, P. J. Love, A. Aspuru-Guzik, and J. L. O'brien, Nature communications 5, 4213 (2014).
- [2] P. J. O'Malley, R. Babbush, I. D. Kivlichan, J. Romero, J. R. McClean, R. Barends, J. Kelly, P. Roushan, A. Tranter, N. Ding, et al., Physical Review X 6, 031007 (2016).
- [3] A. Kandala, A. Mezzacapo, K. Temme, M. Takita, M. Brink, J. M. Chow, and J. M. Gambetta, Nature 549, 242 (2017).
- [4] R. LaRose, A. Tikku, É. O'Neel-Judy, L. Cincio, and P. J. Coles, npj Quantum Information 5, 1 (2019).
- [5] V. Havlíček, A. D. Córcoles, K. Temme, A. W. Harrow, A. Kandala, J. M. Chow, and J. M. Gambetta, Nature 567, 209 (2019).
- [6] M. Schuld and N. Killoran, Physical review letters 122, 040504 (2019).
- [7] S. McArdle, T. Jones, S. Endo, Y. Li, S. C. Benjamin, and X. Yuan, npj Quantum Information 5, 1 (2019).
- [8] K. Mitarai, Y. O. Nakagawa, and W. Mizukami, Physical Review Research 2, 013129 (2020).
- [9] P. W. Shor, Physical Review A **52**, R2493 (1995).
- [10] D. Gottesman, arXiv preprint quant-ph/9705052 (1997).

- [11] S. J. Devitt, W. J. Munro, and K. Nemoto, Reports on Progress in Physics 76, 076001 (2013).
- [12] D. A. Lidar and T. A. Brun, Quantum error correction (Cambridge university press, 2013).
- [13] K. Temme, S. Bravyi, and J. M. Gambetta, Physical review letters 119, 180509 (2017).
- [14] Y. Li and S. C. Benjamin, Physical Review X 7, 021050 (2017).
- [15] X. Bonet-Monroig, R. Sagastizabal, M. Singh, and T. O'Brien, Physical Review A 98, 062339 (2018).
- [16] S. Endo, S. C. Benjamin, and Y. Li, Physical Review X 8, 031027 (2018).
- [17] J. R. McClean, Z. Jiang, N. C. Rubin, R. Babbush, and H. Neven, Nature Communications 11, 1 (2020).
- [18] S. Endo, Z. Cai, S. C. Benjamin, and X. Yuan, arXiv preprint arXiv:2011.01382 (2020).
- [19] A. Lowe, M. H. Gordon, P. Czarnik, A. Arrasmith, P. J. Coles, and L. Cincio, arXiv preprint, arXiv:2011.01157 (2020).
- [20] B. Koczor, arXiv preprint arXiv:2011.05942 (2020).
- [21] W. J. Huggins, S. McArdle, T. E. O'Brien, J. Lee, N. C. Rubin, S. Boixo, K. B. Whaley, R. Babbush, and J. R. McClean, arXiv preprint arXiv:2011.07064 (2020).

- [22] A. Kandala, K. Temme, A. D. Córcoles, A. Mezzacapo, J. M. Chow, and J. M. Gambetta, Nature 567, 491 (2019).
- [23] C. Song, J. Cui, H. Wang, J. Hao, H. Feng, and Y. Li, Science Advances 5 (2019).
- [24] M. Paris and J. Řehàček, eds., Quantum state estimation, Vol. 649 (Springer Science & Business Media, 2004).
- [25] M. R. Geller, Quantum Science and Technology 5 (2020).
- [26] F. B. Maciejewski, Z. Zimborás, and M. Oszmaniec, Quantum 4 (2020).
- [27] E. Haapasalo, T. Heinosaari, and J.-P. Pellonpää, Quantum Information Processing 11, 1751 (2012).
- [28] M. Steffen, M. Ansmann, R. C. Bialczak, N. Katz, E. Lucero, R. McDermott, M. Neeley, E. M. Weig, A. N. Cleland, and J. M. Martinis, Science 313, 1423 (2006).
- [29] Y. Chen, M. Farahzad, S. Yoo, and T.-C. Wei, Physical Review A 100, 052315 (2019).
- [30] B. Nachman, M. Urbanek, W. A. de Jong, and C. W. Bauer, arXiv preprint arXiv:1910.01969 (2019).
- [31] K. E. Hamilton, T. Kharazi, T. Morris, A. J. McCaskey, R. S. Bennink, and R. C. Pooser, in 2020 IEEE International Conference on Quantum Computing and Engi-

- neering (QCE) (2020) pp. 430-440.
- [32] H. Kwon and J. Bae, arXiv preprint arXiv:2003.12314 (2020).
- [33] S. S. Tannu and M. K. Qureshi, in Proceedings of the 52nd Annual IEEE/ACM International Symposium on Microarchitecture, MICRO '52 (Association for Computing Machinery, New York, NY, USA, 2019) p. 279–290.
- [34] R. Hicks, C. W. Bauer, and B. Nachman, arXiv preprint arXiv:2010.07496 (2020).
- [35] S. Bravyi, S. Sheldon, A. Kandala, D. C. Mckay, and J. M. Gambetta, arXiv preprint arXiv:2006.14044 (2019).
- [36] A. Erhard, J. J. Wallman, L. Postler, M. Meth, R. Stricker, E. A. Martinez, P. Schindler, T. Monz, J. Emerson, and R. Blatt, Nature Communications 10, 1 (2019).
- [37] S. T. Flammia and J. J. Wallman, arXiv preprint arXiv:1907.12976 (2019).
- [38] S. Chen, W. Yu, P. Zeng, and S. T. Flammia, arXiv preprint arXiv:2011.09636 (2020).